

# A Compact Dual Band Dual Polarized Monopole Antenna with Enhanced Bandwidth for C, X, and Ku Band Applications

Reshmi Dhara\*

**Abstract**—This article presents a compact, single feed dual-band dual-polarized (DBDP) microstrip antenna. The proposed design involves an inverted Y-shaped radiating patch and a rectangular open-loop positioned near its right corner that creates mutual coupling to attain wideband circular polarization (CP). To achieve enhanced axial ratio bandwidth (ARBW), a semi-rectangular ground plane with two asymmetric truncated L-shaped slots has been used. An L-shaped slotted quarter wave microstrip line feed is used here for broader ARBW and proper impedance matching. The measured dual impedance bandwidths (IBW) in the range 5.85–6.52 GHz (centre resonance frequency  $f_{rc1} = 6.19$  GHz, 10.66%) in lower frequency region and 7.25–13.64 GHz ( $f_{rc2} = 10.445$  GHz, 61.18% bandwidth) in higher frequency region. The two ARBW bands span over 7.22–10.99 GHz ( $f_{c1} = 9.105$  GHz, 41.41%) and 11.67 GHz–12.25 GHz ( $f_{c2} = 11.96$  GHz, 4.85%). The measured peak gains between 3.20 and 4.96 dBi over the entire IBW range makes the LP and CP bands suitable for ITS (5.9 GHz), U-NII-5 of 6 GHz band, some C-band, ITU-8 GHz, some X-band, and Ku-band applications.

## 1. INTRODUCTION

Recently, dual-band dual-polarized (DBDP) antennas have fulfilled multiple requirements of various devices in wireless communication systems. Antennas with omnidirectional radiation are especially useful in personal mobile and global position system (GPS) devices. Conversely, antennas with unidirectional radiation patterns are evolving as an integral technology for numerous communication devices such as global navigation satellite systems, point-to-point communication systems, and other satellite communication systems. A horizontal polarization loop antenna and a vertically polarized monopole antenna are superimposed to produce omnidirectional horizontally/vertically dual-polarized radiation. Presently for communication systems where space is the key interest, multifunctional communication apparatus is required as an alternative to single communication standard apparatus. Because of the attractive features like simpler geometry, low footprint, and light weight, printed monopole antennas serve as one of the most appropriate methodologies. It is well known that a conventional monopole antenna generates linearly polarized (LP) wave in longitudinal direction of the antenna. However, the main disadvantages of LP wave aimed at dual-band operation are multipath fading, low sensitivity to the orientation among the transmitting and receiving antennas, low mobility, etc. [1–3]. This could be overcome to a large extent by using circularly polarized antennas. Hence, dual-band antennas with two different frequency bands simultaneously operating linear and circular polarizations are considerably popular over dual-band antennas with two orthogonal linear polarizations. A multiband antenna with dual polarization characteristics decreases the necessity of multiple antennas. Their CP characteristics also help in effectively combatting multipath interference or fading. To satisfy these requirements of DBDP antennas showing both linear and circular polarizations, different

---

*Received 19 December 2020, Accepted 28 January 2021, Scheduled 5 February 2021*

\* Corresponding author: Reshmi Dhara (reshmidhara@nitsikkim.ac.in).

The author is with the Department of Electronics and Communication Engineering, National Institute of Technology Sikkim, Ravangla, South Sikkim, PIN 737 139, India.

techniques have been utilized by various researchers [4–7]. An asymmetric dipole like radiator coupled with a T-shaped feed line having wide ground plane slot was used [4] to obtain dual-band characteristics. A dual-polarized [5] antenna utilized a printed dipole-like radiator to achieve circular polarization in lower band along with a quasi-Yagi antenna structure to generate end fire LP radiation in the upper band. Additionally, I-shaped resonator (ISR) arrays were used to enhance gain of the antenna. Recently, another group [6] used two planar multiband monopole antennas (using two different substrates, viz. FR4-epoxy and PTFE) to provide LP in lower band and CP in upper band. Another DBDP antenna with single port coplanar waveguide (CPW) feed [7] was designed to obtain LP in lower band and CP in upper band.

Motivated by the above-mentioned works, a simple and compact DBDP monopole antenna with LP in lower band and wide CP in upper band is proposed in this paper. Recently, we designed an inverted Y-shaped monopole antenna [8], which we felt to be one of the best suitable candidates for modification into a DBDP antenna. That previous design could support 5.297–10.460 GHz band and showed a single wide CP band ranging from 6.41 to 8.55 GHz. In order to design a DBDP antenna, we have suitably modified this design in such a way that it can support both linear and circular polarizations.

Intelligent Transport Systems (ITSs) use 5.9 GHz (5.855–5.925 GHz) LP band in Europe and also elsewhere. ITSs provide communication to and from mobile units for mobile service applications. Here mobile service broadcast uses EM wave on a single plane that is why ITS application particularly supports linear polarization. In USA, the unlicensed national information and infrastructure-5 (UNII-5) of 6 GHz bands are allowed for channels 1 to 97, ranging from 5.925 GHz to 6.425 GHz. These bands also use linear polarization for indoor-outdoor applications. On the other hand, the X-band ranging 7.250–7.750 GHz is used for military Fixed Satellite and Mobile Satellite application. The band ranging 7.725–8.500 GHz is used for ITU (8 GHz) application. The band 8.500–10.500 GHz is used for Radiolocation, while 10.525 GHz is used for Microwave motion detector. The band 10.550–10.700 GHz is used for fixed satellite and space research. The Ku-band 11.7–12.2 GHz is used for FSS (Fixed Satellite Service) downlink application. All the above applications need circular polarization wave to support reliable or consistent orientation. We aimed to design an antenna which could have LP in lower band to support ITS and UNII-5 applications and support multifunctional broader circular polarization in higher region.

A very good return loss, wide axial ratio bandwidth, and reliable radiation characteristics are obtained for the proposed antenna. We propose here a DBDP antenna of dimension  $20 \times 20 \text{ mm}^2$  with 26.06% size reduction which is a commendable achievement, making it suitable for small form factor devices. The mutual coupling between a rectangular open loop resonator and an inverted Y-shaped radiator furnished wide CP band. A semi-rectangular ground plane with two asymmetric and truncated L-shaped slots plays a vital role in realizing the higher and lower CP bands within second IBW curve. The quarter wave microstrip feed line was purposefully modified by incorporating a rectangular slot within it to furnish the lower LP band and also widen the lower CP band. These novel design elements helped in obtaining measured dual IBWs from 5.85–6.52 GHz and 7.25–13.64 GHz, and the measured dual ARBWs from 7.22–10.99 GHz and 11.67 GHz–12.25 GHz. This is the widest IBW with wide ARBWs obtained compared to the earlier cited related designs antenna [4–7]. This antenna gives flexibility in dual-band dual-polarization operations in a single device, which is desired for replacing multiple apparatus.

Benchmarking of the proposed antenna with the earlier cited DBDP antennas is presented in Results and Discussions section. It shows that the proposed antenna is more compact and provides wider LP and CP bands.

The paper is structured as follows: Section 2: Antenna Design Procedure; Section 3: Experimental Validations and Discussions; and Section 4: Conclusion.

## 2. ANTENNA DESIGN PROCEDURE

Dual-band dual-polarized (DBDP) antennas can satisfy various functions for different apparatuses. They are extensively utilized in wireless communication systems [9]. In [8], the ARBW was moderate ranging from 6.41 to 8.55 GHz, and the IBW was up to 10.46 GHz. This moderate ARBW range (2.25 GHz) limits the antenna usage in many practical applications, particularly for the wide-band

wireless communications. To overcome this problem, we propose here a DBDP antenna.

The simulated and fabricated structures of the designed antenna are shown in Figs. 1(a), (b) and (c), (d). The footprint of the compact microstrip antenna is only  $20 \times 20 \text{ mm}^2$ . Easily available, the most economically viable FR4-epoxy substrate of 1.6 mm thickness, having  $\epsilon_r = 4.4$  and  $\tan \delta = 0.02$ , is used to fabricate the proposed antenna. The detailed optimized dimension is listed in Table 1.

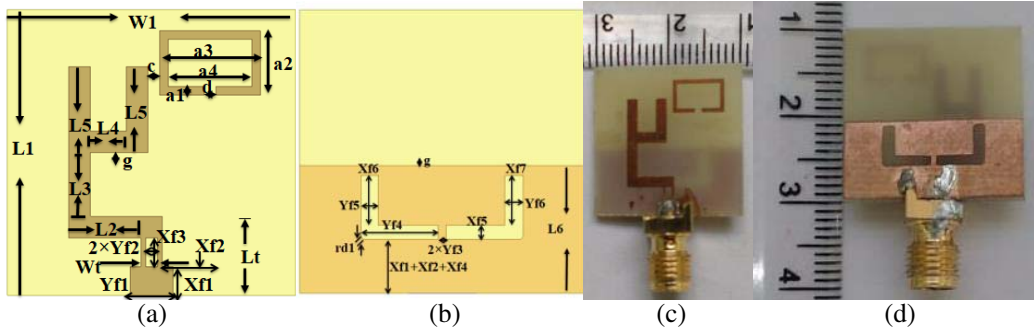


**Figure 1.** Proposed Antenna.2 dimension for (a) simulated top view, (b) simulated bottom view, (b) fabricated top view and (c) fabricated bottom view respectively.

**Table 1.** Optimized dimension of proposed antenna.

Parameter	Value (mm)								
$W1$	20	$L1$	20	$L2$	5	$L3$	4	$L4$	2.5
$L5$	6.5	$L6$	9	$L7$	9	$g$	1	$Lt$	5.5
$Wt$	1.5	$d$	0.6	$a1$	0.6	$a2$	4.5	$c$	0.8
$a3$	7	$a4$	5.8	$h$	1.6	$Xf1$	2	$Xf2$	0
$Xf3$	2	$Xf4$	1.8	$Xf5$	1	$Xf6$	3.5	$Xf7$	3.5
$Yf1$	3	$Yf2$	0.4	$Yf3$	0.3	$Yf4$	5.4	$Yf5$	1.2
$Yf6$	1.3	$rd1$	0.2	-	-	-	-	-	-

The implemented microstrip antenna consists of a main inverted Y-shaped radiating patch with an open loop placed on the right corner of the radiator [10] and an edged ground on the opposite side of the substrate [11]. The evolution steps of the proposed antenna are depicted in Fig. 2. Fig. 3 shows the reflection coefficient and ARBW improvement plots of the implemented antenna. First in Structure.1 a quarter wave  $50 \Omega$  microstrip line feed is used instead of previously used [8] centre feed, for getting additional wide IBW in lower frequency region. This feeding structure gives a better impedance matching network [12] in both lower and higher frequency regions, which results in increase of the IBW in both frequency directions (IBW 5.96–6.59 GHz, 7.45–11.22 GHz and ARBW 7.11–8.4 GHz). The quarter wave microstrip feeding line is used to resonate at 5.8 GHz. Tuning the length of this quarter wave portion for the L-shaped transmission line to  $L2 + Wt + Xf3 = (5 + 1.5 + 2) \text{ mm} = 8.5 \text{ mm}$  generates the LP wave. To get a resonance near 5.8 GHz, the approximate length of the quarter wave transmission line is 7.87 mm ( $\lambda_g/4$ ), which is nearly equal to 8.5 mm ( $0.27\lambda_g$ ,  $\lambda_g =$  guided wavelength at 5.8 GHz). To further increase the ARBW at higher region, two optimized symmetrical rectangular slots are etched from ground plane to give Structure.2. These slots create additional current [13, 14] paths which increase IBW as well as ARBW compared to previous step. However, the generated ARBW was not wide enough (IBW 6.01–6.66 GHz, 7.53–11.39 GHz and ARBW 7.06–8.76 GHz). So, further modifications of the feed and ground plane were contemplated. In the next step for increasing the ARBW, two asymmetric optimized L-shaped slots (vertical slot width for the left slot =  $Yf5 = 1.2 \text{ mm} = 0.038\lambda_g$  and right slot =  $Yf6 = 1.3 \text{ mm} = 0.041\lambda_g$ ) were imprinted on the ground plane [15, 20] to create Structure.3 which

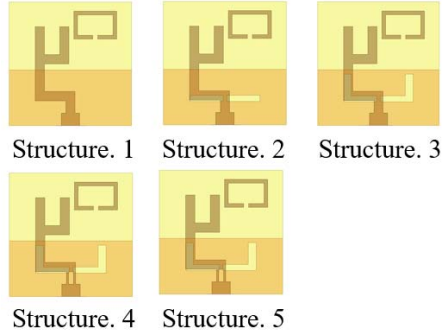


**Figure 2.** Evolution of proposed antenna.

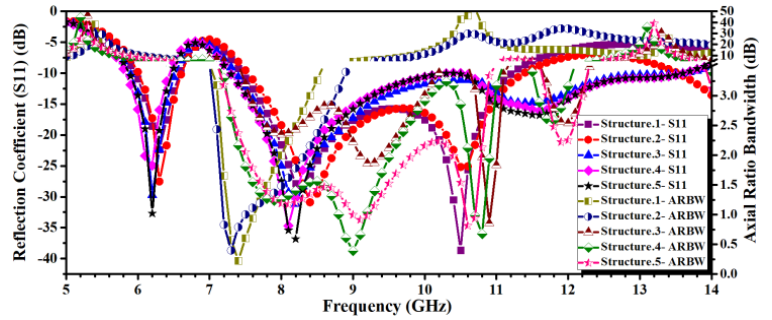


**Figure 3.** Comparison of simulated reflection coefficient and axial ratio for Structure.1-5.

gave three small CP bands inside the IBW (IBW 5.89–6.52 GHz, 7.36–13.6 GHz and ARBW 7.56–10.0 GHz, 10.71–11.08 GHz, 11.75–12.19 GHz). Only a smaller portion ranging 10 GHz–10.71 GHz still did not satisfy 3 dB criteria. So, to achieve wide CP, additional current path was needed to be created on that region so that it satisfied 3 dB criteria. It can be achieved by adding slit [16] or etching slot [17, 21] from the feed line. We chose to use a slot on the feed line to give Structure.4. By incorporating the slot (area =  $2 \times Yf2 \times Xf3 = 0.8 \times 2 \text{ mm}^2 = 0.051\lambda_g^2$ ) in the feed structure, new coupling paths between the patch and slotted ground plane could be generated. Therefore, the number of resonances can be regulated, and it generates a wider bandwidth (IBW 5.83–6.44 GHz, 7.29–10.33 GHz, 10.50–13.61 GHz and ARBW 7.24–10.06 GHz, 10.45–10.99 GHz, 11.58–11.96 GHz) than the feed line without slot. As a result, the portion not satisfying 3 dB criteria got reduced to a smaller range (10.06 GHz–10.45 GHz). Therefore, to get ARBW in the entire range, the electric field needed to be perturbed with orthogonal phase difference and equal amplitude on that small region. Finally, Structure.5 was obtained by using two truncated (truncated etching isosceles right triangle area =  $0.5 \times rd1 \times rd1 = 0.02 \text{ mm}^2 = 6.35 \times 10^{-4} \lambda_g^2$ ) L-shaped slots [18, 19]. Structure.5 gave two wide impedance bands, one linearly polarized band in lower frequency region and the other in higher frequency region containing two wide circularly polarized bands (IBW 5.88–6.48 GHz, 7.29–13.62 GHz and ARBW 7.24–10.87 GHz, 11.70–12.20 GHz). Since it fulfilled our aim, we decided to fabricate this Structure.5 and test its performance.

### 3. RESULTS AND DISCUSSIONS

Ansys Electronics Desktop 2020 R1 was used for simulations. Agilent Technologies, PNA-L Network Analyzer-N5234A (10 MHz–43.5 GHz) VNA has been used to perform the IBW measurement.

The proposed antenna covered the measured IBW from 5.85–6.52 GHz ( $f_{rc1} = 6.19 \text{ GHz}$ , 10.66%) and 7.25–13.64 GHz ( $f_{rc2} = 10.445 \text{ GHz}$ , 61.18% bandwidth), and the simulated IBW covered the ranges 5.88–6.48 GHz ( $f_{rc1} = 6.18 \text{ GHz}$ , 9.71%) and 7.29–13.62 GHz ( $f_{rc2} = 10.45 \text{ GHz}$ , 60.54%) shown in Fig. 4(a).

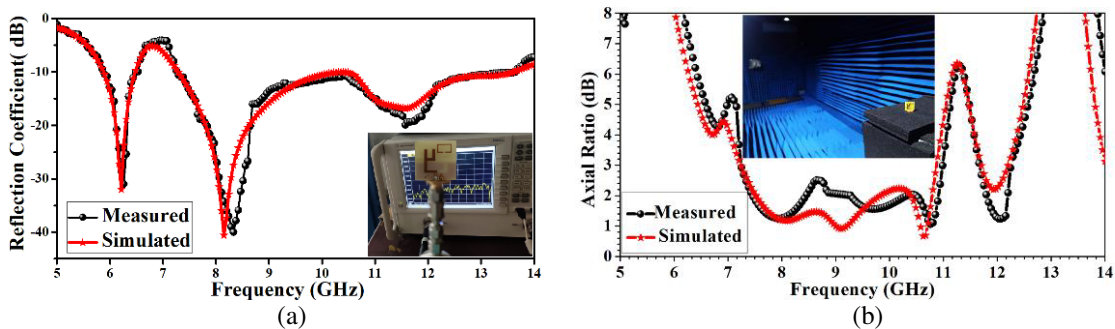


**Figure 4.** Comparison of measured and simulated (a) reflection coefficient curves and (b) ARBW curves.

Figure 4(b) depicts the comparison between measured and simulated ARBW of the implemented antenna. The measured ARBW spans over 7.22–10.99 GHz ( $f_{c1} = 9.105$  GHz, 41.41%) and 11.67 GHz–12.25 GHz ( $f_{c2} = 11.96$  GHz, 4.85%), while the simulated ARBW spans over 7.24–10.87 GHz ( $f_{c1} = 9.05$  GHz, 40.09%) and 11.7 GHz–12.2 GHz ( $f_{c2} = 11.95$  GHz, 4.18%). Both the CP bands are inside the measured and simulated IBWs. Therefore, the proposed DBDP antenna can be used for ITS-5.9 GHz (5.855–5.925 GHz) and U-NII-5 (6 GHz for channels 1 to 97, 5.925 GHz to 6.425 GHz) in lower impedance band for LP application. In higher impedance for CP application, the implemented antenna can be used for X-band (7.250–7.750 GHz) military Fixed Satellite and Mobile Satellite application, ITU-8 GHz (7.725–8.500 GHz) application, Radiolocation (8.500–10.500), Microwave motion detector (10.525 GHz), Fixed satellite and space research (10.550–10.700 GHz), Ku-band (11.7–12.2 GHz) FSS (Fixed Satellite Service) downlink application.

Figure 5(a) depicts the measured and simulated radiation efficiencies for the implemented antenna with respect to frequency. The measured radiation efficiencies are in the range of 78%–90% for both the impedance bands, and the measured efficiency is maximum at 8.46 GHz, 90.26%. Fig. 5(a) also shows the measured and simulated peak gains. The measured gain is in the range of 3.20–4.96 dBi for both the impedance bands, and the maximum measured peak gain is 4.96 dBi at 12.51 GHz.

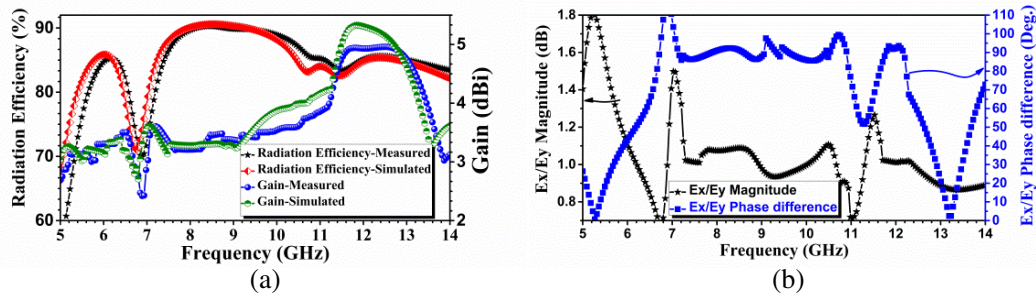


**Figure 5.** Implemented antenna (a) Measured, simulated Gain and Radiation Efficiency plot vs. Frequency, (b) Simulated  $E_x/E_y$  magnitude and phase plot vs. Frequency.

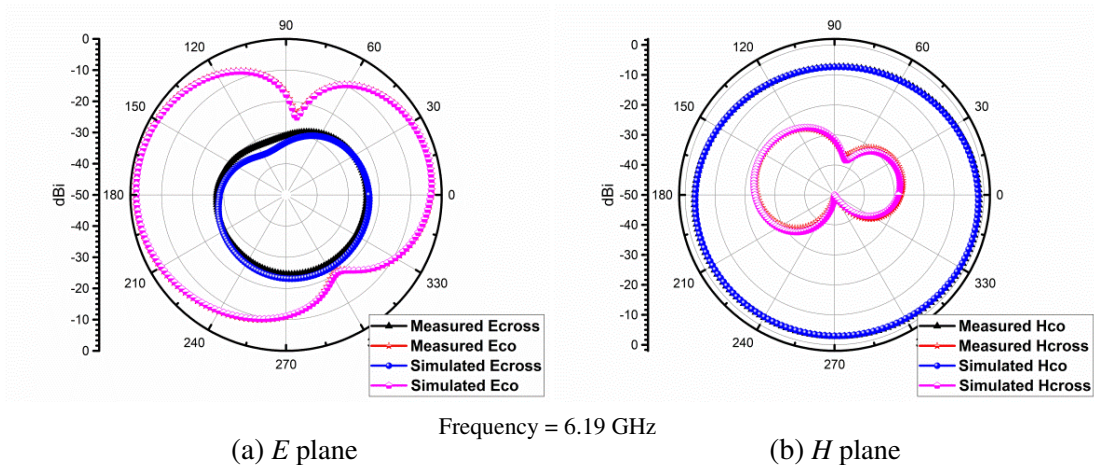
Figure 5(b) shows that the magnitude of  $E_x/E_y$  is nearly equal to 1 or 0 dB over the range of dual CP bands, and the phase difference between them is also around  $90^\circ$ . This proves that the dual bands satisfy CP criteria.

Figure 6(a) shows the simulated electric field radiation pattern of the proposed antenna at the frequency  $f_{rc1} = 6.19$  GHz for  $E_{co}$  (elevation plane,  $XZ$  plane,  $\theta = 90^\circ$ ) plane and  $E_{cross}$  (azimuth plane,  $XY$  plane,  $\theta = 0^\circ$ ) plane. It proves that the radiation pattern for  $E$ -field is omnidirectional like a conventional dipole mode antenna. Fig. 6(b) shows the simulated magnetic field radiation pattern of the proposed antenna for  $H_{co}$  (azimuth plane,  $XY$  plane,  $\varphi = 0^\circ$ ) plane and  $H_{cross}$  (Elevation plane,  $XY$  plane,  $\varphi = 90^\circ$ ). Here the cross-polarization radiations are less than co-polarization by an amount of 26 dBi.

Simulated and measured radiation patterns for LHCP and RHCP are observed in Figs. 7(a), (c) and (b), (d) at  $\varphi = 0^\circ$  ( $XZ$  plane) and  $\varphi = 90^\circ$  ( $YZ$  plane) at  $f_{c1} = 10.45$  GHz and  $f_{c2} = 11.96$ . It is found at CP resonating frequencies on the broadside direction that the radiations are RHCP while the measured co-polarizations are greater than cross-polarization levels by 23 dBi and 37 dBi, respectively. Due to the asymmetric Y-shaped patch, the current distribution in it is constructive for the reason that radiation is slightly tilted from its broadside direction.

From the simulated normalized distribution of currents, it was found that for four different time instants ( $t = 0$ ,  $t = T/4$ ,  $t = 3T/4$ ,  $t = T$  where  $T$  is the time period), CP modes can be achieved at  $f_{c1} = 10.45$  GHz,  $f_{c2} = 11.96$  GHz which are RHCP.

Finally, relative benchmarking of the proposed antenna with the recently reported DBDP antennas has been attempted. Their year of publication, performance parameters like antenna size, polarization, impedance bandwidth (%), AR bandwidth (%), and center frequency of CP band (GHz) are summarized in Table 2.



**Figure 6.** Simulated radiation pattern of the proposed antenna for (a) Eco (Elevation plane,  $XZ$  plane,  $\theta = 90^\circ$ ) plane and Ecross (Azimuthal plane,  $XY$  plane,  $\theta = 0^\circ$ ) plane, (b) Hco (Azimuthal plane,  $XY$  plane,  $\varphi = 0^\circ$ ) plane and Hcross (Elevation plane,  $XY$  plane,  $\varphi = 90^\circ$ ) plane.

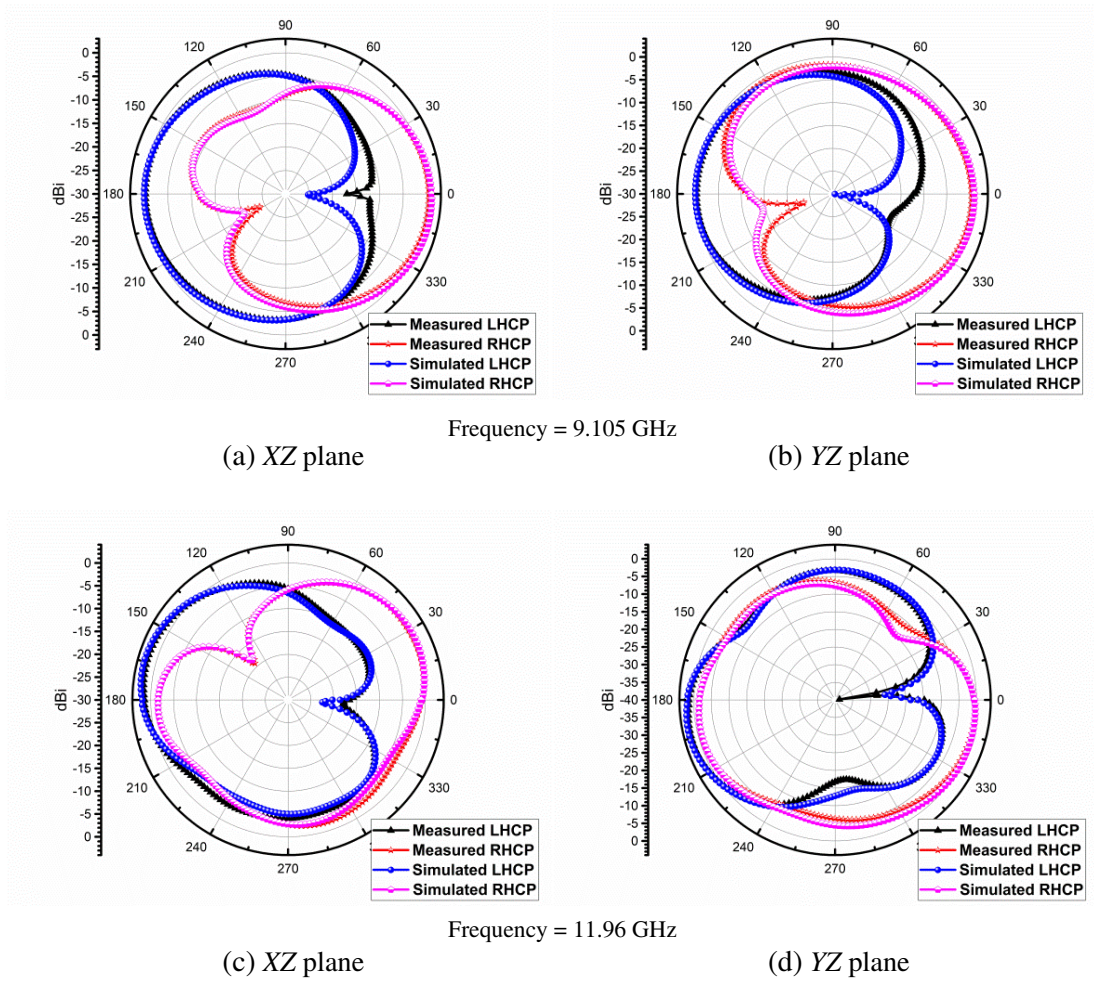


**Figure 7.** Simulated and measured radiation patterns for (LHCP and RHCP) in the (a), (c)  $XZ$  ( $\varphi = 0^\circ$ ) and (b), (d)  $YZ$  ( $\varphi = 90^\circ$ ) planes.

**Table 2.** Comparison with related DBDMDP antennas with proposed antenna.

References (Year)	Antenna size (mm <sup>3</sup> )	Polarization	IBW (%)	$f_{rc}$ (GHz)	ARBW (%)	$f_c$ (GHz)
4 (2011)	45 × 50 × 1.57	RHCP; LP	74; 39	2.725; 7.15	16	2.35
5 (2017)	38 × 32.5 × 1.57	RHCP; LP	3.93; 29.45	5.845; 8.08	2.57	5.84
6 (2019)	50 × 35 × 1.6	LP; LHCP	20.57; 68.74	2.43; 7.39	18.5	5.675
7 (2020)	30 × 30 × 1.6	RHCP; LP	30.43; 14.94	4.6; 8.1	27.89	4.66
<b>Proposed Antenna</b>	<b>20 × 20 × 1.6</b>	<b>LP; RHCP</b>	<b>10.66; 61.18</b>	<b>6.19; 10.445</b>	<b>41.41; 4.85</b>	<b>9.105; 11.96</b>

#### 4. CONCLUSION

A DBDP antenna with enhanced dual CP bandwidth in the higher frequency and an LP band in the lower frequency region is realized by implementing modifications in ground plane and feeding network of an inverted Y-shaped monopole antenna. A semi-rectangular ground plane with two asymmetric and truncated L-shaped slots helped in achieving higher and lower CP bands within second IBW curve. The quarter wave microstrip feed line and rectangular slot within it furnished the LP band and wider lower CP band within second impedance band, respectively. The compact (size  $20 \times 20 \text{ mm}^2$ , i.e.,  $0.635 \times 0.635 \lambda_g^2$ ,  $\lambda_g =$  guided wavelength at 5.8 GHz, 26.06% size reduction) proposed antenna gives wide dual IBWs, one at lower frequency region 5.86–6.52 GHz and the other at higher frequency region 7.25–13.64 GHz. The dual-polarized bands are at lower frequency region LP (10.66% at 6.19 GHz) and at higher frequency region two CP bands (41.41% at 9.105 GHz and 4.85% at 11.96 GHz). The implemented antenna can support C, X, and Ku band applications in a single small form factor device. This DBDP antenna is the most compact and gives the widest dual CP and LP bands among the recently reported designs.

#### 5. SUPPLEMENTARY DOCUMENT

Simulated surface current distribution, effect of VSWR over IBW using Smith chart, parametric studies, 3 dB axial ratio mechanism and for proposed the antenna are presented in supplementary document.

#### ACKNOWLEDGMENT

I sincerely thank Dr. Sanjeev Yadav, Head, Department of ECE, Government Women Engineering College Ajmer, Rajasthan, India for carrying out the measurements.

#### REFERENCES

1. Toh, B. Y., R. Cahill, and V. F. Fusco, "Understanding and measuring circular polarization," *IEEE Transactions on Education*, Vol. 46, No. 3, 313–318, 2003, DOI: 10.1109/TE.2003.813519.
2. Yu, D., S. X. Gong, Y. Xu, and Y. T. Wan, "Dual-band dual-polarized circular microstrip patch antenna with the curved slots on the ground," *Progress In Electromagnetics Research Letters*, Vol. 51, 27–31, 2015.
3. Langston, W. L. and D. R. Jackson, "Impedance, axial-ratio, and receive-power bandwidths of microstrip antennas," *IEEE Transactions on Antennas and Propagation*, Vol. 52, No. 10, 2769–2774, 2004.
4. Bao, X. L. and M. J. Ammann, "Wideband dual-frequency dual-polarized dipole-like antenna," *IEEE Antennas and Wireless Propagation Letters*, Vol. 10, 831–834, 2011, DOI: 10.1109/LAWP.2011.2164609.

5. Ding, K., C. Gao, Y. Wu, D. Qu, B. Zhang, and Y. Wang, "Dual-band and dual-polarized antenna with endfire radiation," *IET Microwaves, Antennas & Propagation*, Vol. 11, No. 13, 1823–1828, 2017, DOI: 10.1049/iet-map.2017.0124.
6. Bag, B., P. Biswas, S. Biswas, and P. P. Sarkar, "Wide-bandwidth multifrequency circularly polarized monopole antenna for wireless communication applications," *International Journal of RF and Microwave Computer-Aided Engineering*, Vol. 29, No. 3, e21631, 2019, DOI: 10.1002/mmce.21631.
7. Madaka, K. C. R. and P. Muthusamy, "Mode investigation of parasitic annular ring loaded dual band coplanar waveguide antenna with polarization diversity characteristics," *International Journal of RF and Microwave Computer-Aided Engineering*, e22119, 2020, DOI: 10.1002/mmce.22119.
8. Dhara, R. and T. Kundu, "A compact inverted Y-shaped circularly polarized wideband monopole antenna with open loop," *Engineering Reports*, 2020, DOI: 10.1002/eng2.12326.
9. Lin, J., Z. Qian, W. Cao, S. Shi, Q. Wang, and W. Zhong, "A low-profile dual-band dual-mode and dual-polarized antenna based on AMC," *IEEE Antennas and Wireless Propagation Letters*, Vol. 16, 2473–2476, 2017, DOI: 10.1109/LAWP.2017.2724540.
10. Dhara, R., S. Yadav, M. M. Sharma, S. K. Jana, and M. C. Govil, "A circularly polarized quad-band annular ring antenna with asymmetric ground plane using theory of characteristic modes," *Progress In Electromagnetics Research M*, Vol. 100, 51–68, 2021.
11. Tan, M. T. and B. Z. Wang, "A dual-band circularly polarized planar monopole antenna for WLAN/Wi-Fi applications," *IEEE Antennas and Wireless Propagation Letters*, Vol. 15, 670–673, 2015, DOI: 10.1109/LAWP.2015.2466596.
12. Chen, Y. Y., Y. C. Jiao, G. Zhao, F. Zhang, Z. L. Liao, and Y. Tian, "Dual-band dual-sense circularly polarized slot antenna with a C-shaped grounded strip," *IEEE Antennas and Wireless Propagation Letters*, Vol. 10, 915–918, 2011, DOI: 10.1109/LAWP.2011.2166750.
13. Singh, A. K., S. Patil, B. K. Kanaujia, and V. K. Pandey, "A novel printed circularly polarized asymmetric wide slot antenna for digital cellular system," *Microwave and Optical Technology Letters*, Vol. 62, No. 3, 1438–1447, 2020, DOI: 10.1002/mop.32177.
14. Ellis, M. S., F. B. Effah, A. R. Ahmed, J. J. Kponyo, J. Nourinia, C. Ghobadi, and B. Mohammadi, "Asymmetric circularly polarized open-slot antenna," *International Journal of RF and Microwave Computer-Aided Engineering*, Vol. 30, No. 5, e22141, 2020, DOI: 10.1002/mmce.22141.
15. Dhara, R., "Quad-band circularly polarized CPW-fed G-shaped printed antenna with square slot," *Radioelectronics and Communications Systems*, Vol. 63, No. 7, 376–385, 2020, DOI: 10.20535/S0021347020070055.
16. Pourahmadazar, J., C. Ghobadi, J. Nourinia, N. Felegari, and H. Shirzad, "Broadband CPW-fed circularly polarized square slot antenna with inverted-L strips for UWB applications," *IEEE Antennas and Wireless Propagation Letters*, Vol. 10, 369–372, 2011, DOI: 10.1109/LAWP.2011.2147271.
17. Shokri, M., V. Rafei, S. Karamzadeh, Z. Amiri, and B. Virdee, "Miniaturised ultra-wideband circularly polarised antenna with modified ground plane," *Electronics Letters*, Vol. 50, No. 24, 1786–1788, 2014, DOI: 10.1049/el.2014.3278.
18. Fujimoto, T., Y. Yoshitake, and D. Yagyu, "Design and simulation based studies of a dual-band circularly-polarized square microstrip antenna," *Progress In Electromagnetics Research Letters*, Vol. 52, 129–134, 2015.
19. Saini, R. K. and P. S. Bakariya, "Dual-band dual-sense circularly polarized asymmetric slot antenna with f-shaped feed line and parasitic elements," *Progress In Electromagnetics Research M*, Vol. 69, 185–195, 2018.
20. Dhara, R., S. K. Jana, and M. Mitra, "Tri-band circularly polarized monopole antenna for wireless communication application," *Radioelectronics and Communications Systems*, Vol. 63, No. 4, 213–222, 2020, DOI: 10.3103/S0735272720040044.
21. Dhara, R. and M. Mitra, "A triple-band circularly polarized annular ring antenna with asymmetric ground plane for wireless applications," *Engineering Reports*, Vol. 2, No. 4, e12150, 2020, DOI: 10.1002/eng2.12150.